

Vision-Based Mobile Robot Speed Control Using a Probabilistic Occupancy Map

Yoshiro Negishi, Jun Miura, and Yoshiaki Shirai
Department of Computer-Controlled Mechanical Systems
Osaka University, Suita, Osaka 565-0871, Japan
{negishi,jun,shirai}@cv.mech.eng.osaka-u.ac.jp

Abstract

This paper describes a method of controlling the robot speed using a probabilistic occupancy map. It is usually necessary for a robot to make sure that a target region is free before entering there. If the robot is not confident the state (free or occupied) of the region, the robot has to make enough observations to be confident. If the distance to the region is long, the robot can expect to have enough observations until reaching there. If the distance is short, however, the robot may have to slow down for making enough observations. Based on this consideration, we develop a method for controlling the robot speed by considering the state of a target region. The method is applied to our mobile robot with an omnidirectional stereo and a laser range finder. The robot successfully moved around in an unknown environment with adaptively controlling its speed.

1 Introduction

Mobile robot navigation in unknown environments has been one of the active research areas in robotics. Many researches focus on generating a reliable map from uncertain data obtained by internal (e.g., odometry) and external (e.g., vision and sonar) sensors [3, 5, 9]. The main objective of these researches is to generate an accurate map as possible. Some dealt with observation (or motion) planning issues; in these researches, the plan has been made for increasing the quality of the map (e.g., [1]) or for exploring the unobserved spaces (e.g., [2]), not for efficient navigation.

This paper is, different from the previous works, concerned with realizing an efficient navigation in unknown environments. In the case of mobile robots, efficiency depends on the path and the speed it takes. Among these two factors, we focus on the speed control.

Moon et al. [7] proposed to control the speed based on the size of the nearby free space considering the uncertainty of motion and visual localization. They treated the tradeoff between the safety and the efficiency. That is, a fast movement is efficient but may be unsafe due to a large cumulative motion uncertainty; on the other hand, a slow movement is safe

because many observations can be made but is not efficient. They proposed a safety criterion to check if the current speed is safe for the nearby free space, and selected the maximum safe speed. Although their method dealt with only completely known environments, the basic idea of considering the trade-off can be applied to our problem of determining the speed based on a partially uncertain map.

It is usually necessary for a robot to make sure that a target region is free before entering there. Therefore, in order to move into a region which has not been certainly determined as free, the robot needs further observations of the region. If the distance to such an undecided region is long, the robot can expect to observe it many times and, therefore, to have a confident interpretation of the region until the robot reaches the region, even if the robot moves relatively fast. If the distance is short, on the other hand, the robot may have to reduce the speed in order to make an enough number of observations before reaching there. Based on this consideration, we propose to control the robot speed using the distance to the undecided region which the robot moves into next. Using this method, we can realize a robot motion of slowing down near an uncertain area such as the one beyond a corner or the one where enough range information has not been obtained so far; such a motion is exactly the same as what we do in walking through (partially) unknown environments.

We experimentally test the proposed control method using our mobile robot with an omnidirectional stereo and a laser range finder (see Fig. 1). We use a map generation method [6] which generates a free space map by integrating two probabilistic occupancy maps for both sensors.

2 Speed Control Using a Safety Criterion

This section explains the outline of our method for determining the robot speed from a map describing free spaces, obstacle regions, and undecided regions.

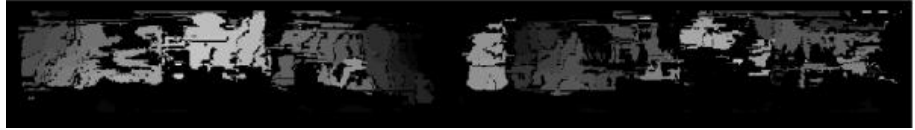
Fig. 2 illustrates an example situation where as a robot moves forward, the *free* region expands in the same direction with the accumulation of newly observed data. In order to be confident with the vacancy of a currently-unknown region (called an *undecided region*), the robot needs to observe it several times due to observation uncertainties. If the distance



(a) Input omnidirectional image (lower camera).



(b) Panoramic image converted from (a).



(c) panoramic disparity image obtained from (b).

Figure 3. Omnidirectional stereo generates a panoramic disparity image.

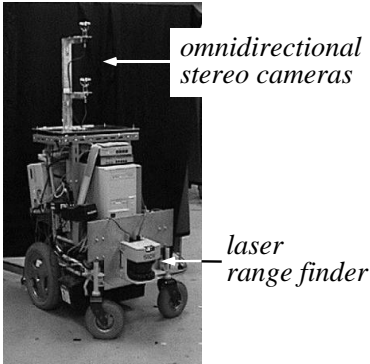


Figure 1. Our mobile robot.

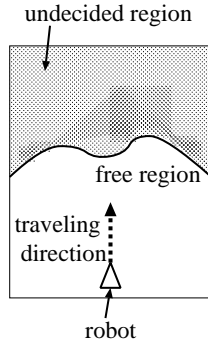


Figure 2. Free and undecided regions.

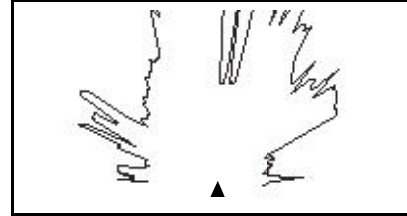


Figure 4. An example LRF measurement. The black triangle indicates the position and the direction of the robot.

to the region is long, the robot expects to make an enough number of observations to be confident until it reaches there. If the distance is short, however, the robot needs to move slowly so that it can sufficiently observe the region. We apply the strategy of selecting the *fastest safe speed* to this situation.

We first define a safety criterion for judging whether a speed is safe. Let N be the minimum number of observations of an undecided region required to enter there. Also let d be the distance to the region and T be the time for one observation (considered to be constant). Since the robot has to observe at least N times before traveling by distance d , the safety criterion is:

$$\frac{d}{vT} \geq N, \quad (1)$$

where v is a robot speed; speed v is safe if this inequality holds. Then, the fastest safe speed v_{max} is:

$$v_{max} = \frac{d}{NT}. \quad (2)$$

If v_{max} is larger than the robot's fastest speed v_{max}^r , the robot moves at v_{max}^r ; otherwise it moves at v_{max} .

To adopt this speed control method, we need to determine N and d . N is determined by considering the observation and the map uncertainty model. Sec 4.4 explains how to determine N from the models. d is the length of a safe path, which is the result of a path planning described in Sec. 5.

3 Two Range Sensors

3.1 Real-time Omnidirectional Stereo

The stereo system uses a pair of vertically-aligned omnidirectional cameras (see Fig. 1). The input images are converted to panoramic images, in which epipolar lines become vertical and in parallel; thus, efficient stereo matching algorithms for the conventional stereo configuration can be applied. The system can generate the disparity image of 360x50 in size and 40 in disparity range in every 0.18[s] Fig. 3 shows the panoramic conversion and disparity calculation. In the disparity image (bottom right), larger disparities (nearer points) are drawn in brighter color. Since the objective of mapping is to recognize the free space, we extract the nearest obstacle in each direction. Refer to [4] for the detail.

3.2 Laser Range Finder (LRF)

We use a SICK laser range finder (LRF), which is set at the front of the robot so that it scans the horizontal plane at the height of 35 [cm] from the floor (see Fig. 1). The resolution used is 1.0 [deg] per point (i.e., 181 measurements for 180 degrees). The accuracy of each measurement is ± 5 [cm]. Fig. 4 shows the line of measurements corresponding to the scene shown in Fig. 3.

4 Map Generation by Integrating Two Sensors

This section briefly describes a map generation method used in this research. The method was originally developed in

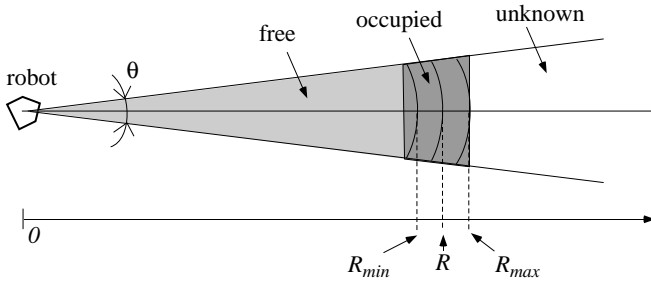


Figure 5. Determination of grid attributes.

[6], which generates a free space map by integrating two probabilistic occupancy maps for the two kinds of sensors. We have slightly modified the original map generation method to discriminate the following two cases; a grid's occupancy is undecided because (1) enough observation has not been made yet or (2) enough information has not been obtained although enough observation has been made. This modification will be explained in Sec. 4.4. Refer to [6] for the detail of the original method.

4.1 Temporal integration of sensor data

We use as a map a probabilistic occupancy grid representation [3]. To integrate the uncertain data, we use *forward sensor model*[8] which describes the physics of the environment, from causes (occupancy) to effects (measurements). We also adopt the *independence assumption*; i.e., update the probability of a grid independently of other grids. This assumption seems reasonable when each sensor has a fairly fine angular resolution.

4.2 Interpretation of range data and integration formula

From one observation, we determine the attribute of each grid; possible attributes are: *occupied*, *free*, and *unknown* (see Fig. 5). The figure shows the attribute determination for a region within one angular resolution. R is the observed distance (by omnidirectional stereo or LRF) to the nearest obstacle, and R_{min} and R_{max} indicate the uncertainty in range measurement¹. The region between R_{min} and R_{max} is labeled as *occupied*. The region before the occupied region is labeled as *free*. The region behind the occupied region is labeled as *unknown*. In the case of stereo, all regions corresponding to the directions in which any obstacles are not detected (possibly due to the failure of stereo matching) are labeled as *unknown*.

Let O be the event that an obstacle is detected. O occurs at *occupied* grids; the inverse event \bar{O} occurs at *free* grids. For such grids, the update of the probability is carried out as follows.

Let E be the event that an obstacle exist, and let $P(E)$ be the probability that an obstacle exist (at a grid). The new probability map to be obtained by integrating a new observation is

¹Refer to [4] for the uncertainty estimate of omnidirectional stereo. The uncertainty in LRF measurement is constant regardless of the measured value.

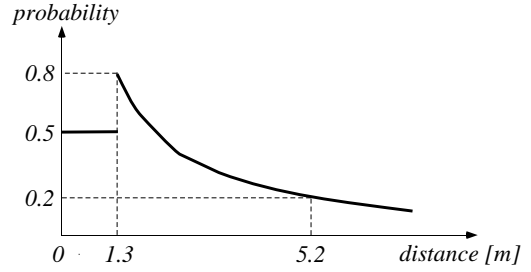


Figure 6. Stereo uncertainty model, $P(O|E)$.

given by the conditional probabilities: $P(E|O)$ and $P(E|\bar{O})$. These probabilities are calculated by the Bayes' theorem as follows:

$$P(E|O) = \frac{P(O|E)P(E)}{P(O|E)P(E) + P(O|\bar{E})P(\bar{E})}, \quad (3)$$

$$P(E|\bar{O}) = \frac{P(\bar{O}|E)P(E)}{P(\bar{O}|E)P(E) + P(\bar{O}|\bar{E})P(\bar{E})}, \quad (4)$$

where $P(E)$ is the prior probability and \bar{E} is the proposition that an obstacle does not exist. Among the terms in the above equations, $P(O|E)$ and $P(O|\bar{E})$ are observation models described below; $P(\bar{O}|E) = 1 - P(O|E)$; $P(\bar{O}|\bar{E}) = 1 - P(O|\bar{E})$; $P(\bar{E}) = 1 - P(E)$. Integration for each grid is performed independently of the others (*the independence assumption*).

4.3 Probabilistic models of sensor uncertainty

4.3.1 Stereo uncertainty model

$P(O|E)$ is the probability that an obstacle is observed when it actually exists. In the case of stereo, the possibility of incorrect matches is considered to rise as an obstacle becomes distant and its size in the image decreases. Since the size is inversely proportional to the distance, we assume that $P(O|E)$ is also inversely proportional to the distance. Fig. 6 shows the definition of $P(O|E)$ for stereo, which is constructed by considering the observable range of the omnidirectional stereo and the experimental results. $P(O|\bar{E})$ corresponds to the case where a false object is detected due to a false stereo matching, and is set to 0.05.

4.3.2 LRF uncertainty model

The measurement of the LRF is fairly reliable and the reliability does not depend on the distance to obstacles. Therefore we set $P(O|E)$ to 0.9 and $P(O|\bar{E})$ to 0.05.

4.4 Integration of two maps

The two probabilistic grid maps are integrated as follows. Since the two sensors may detect different parts of an object, a direct integration of probability values is not appropriate [6]. We therefore first classify each grid of a map into four classes and then integrate the classification result into the final free space map.

Table 1. The integration rule.

OB: obstacle FS: free space

UD_{wt}: undecided with observation

UD_{wo}: undecided without observation

		stereo			
		OB	UD _{wo}	UD _{wt}	FS
L	OB	OB	OB	OB	OB
R	UD _{wo}	OB	OB	OB	OB
F	UD _{wt}	OB	OB	OB	FS
	FS	OB	OB	FS	FS

We use two thresholds for the first classification. If the occupancy probability of a grid is larger than the higher threshold (currently, 0.7), the grid is classified as *obstacle*; if the probability is less than the lower threshold (currently, 0.2), the grid is classified as *free space*; otherwise, classified as *undecided*. This classification into three was used in the original version [6]. In this paper, we further classify *undecided* into two classes.

The second classification is for discriminating the following two cases. (1) The occupancy of a grid is undecided because enough information has not been obtained although the robot observes there many times. A typical situation is that the omnidirectional stereo cannot obtain range data for textureless objects. For a grid in the direction of such an object, its class remains *undecided* even if the stereo tries to observe the object many times. In this case, we believe in the LRF's interpretation. (2) The occupancy is undecided because enough observation has not been made yet. Since we use a probabilistic uncertainty model and integrate observations statistically, each sensors needs some observations to determine the occupancy of a grid with confidence (i.e., free space or obstacle). Therefore, if the number of observations of a grid is small, we have to wait until the situation becomes clearer by further observing it. We discriminate the two cases using a threshold for the number of observations. If the number is larger than the threshold (case (1)), we classify a grid as *undecided with observation*; otherwise *undecided without observation*. The number of observations is incremented when a grid has event O or \bar{O} (see Sec. 4.2), or when a grid is in the direction for which any range measurement is not obtained.

To determine the threshold for the number of observations, we examine how the occupancy probability changes as more observations are obtained, using the observation uncertainty models and the probabilistic integration rules. A typical examination result is that if the robot is initially 500[cm] distant from a front object, and if the robot moves at 50[cm/frame] while observing the object using stereo, five observations are needed to make the grids in front of the object be classified as free. From this and other examination results, we currently use five as the threshold for stereo. In a similar way, we determined to use one as the threshold for LRF.

These thresholds for the number of observations are based on an optimistic prediction that the front object is always properly observed. If at least one out of five observations (in the case of stereo) fails due to some reason, the state of the grids in front of the object may not be determined as

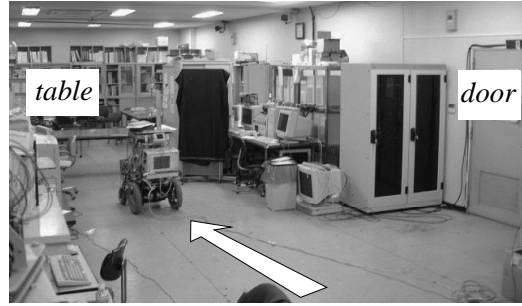


Figure 7. An example scene.

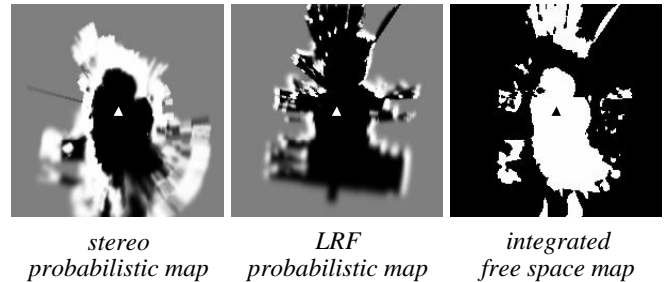


Figure 8. Probabilistic maps and a free space map. Black and white triangles indicate the robot position and orientation.

free. In such a case, however, since the distance to the undecided region becomes shorter than expected and, therefore, the robot speed is controlled accordingly, the robot can still move safely.

After the classification, the robot integrates the two classification results from both sensors into the free space map using the rule shown in Table 1. The classification and integration processes are carried out *every frame*, after updating both probabilistic maps. The resultant free space map is used for the path planning of the mobile robot.

4.5 Map generation example

Fig. 7 shows an example scene where the robot moved along the arrow. Fig. 8 shows the maps generated after the movement. In the probabilistic maps, brightness indicates the probability. The maps are drawn in the robot coordinates. The table in front of the robot was correctly recognized by the stereo, while the LRF only detected only its legs. On the other hand, the recognition by the stereo of the region near the door on the right failed at many positions because features are scarce on the door, while the LRF correctly recognized the region. In spite of recognition failures by one of the sensors at several positions, the integrated map reasonably represents the free space.

5 A Heuristic Path Planner

This section explains a heuristic motion planner used for determining a safe path towards a destination. The robot keeps a local free space map around the robot. We give the

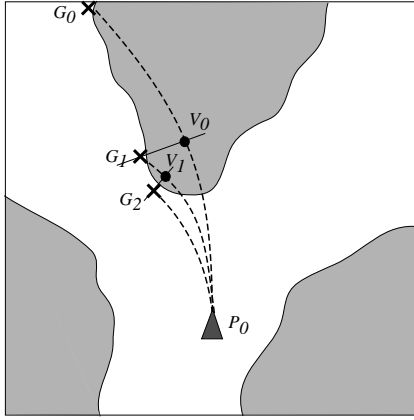


Figure 9. Find a feasible via point. Gray regions indicate obstacles.

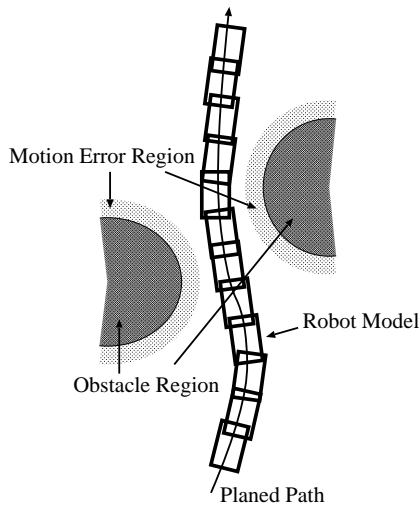


Figure 10. Safety check of a path.

robot the destination in the world coordinates. If the destination is in the local map, the robot use it for path planning. Otherwise, the robot selects a temporary destination which is in the free space and nearest to the given destination, and uses it for path planning. Since our robot is driven by two powered wheels, it always moves on a circular path. So the planner searches for a sequence of safe circular paths among free spaces.

Fig. 9 illustrates the process of path planning by our planner. First the planner searches for a circular path which connects the current position and the destination and whose tangent line at the current position is the same as the current orientation of the robot (arc $P_0 V_0 G_0$ in the figure). If this path is safe, it is selected. Otherwise, the planner first searches for the point on the circular path which is farthest from the free space (V_0 is selected) and draws a line perpendicular to the tangent line of the circular path there, and selects another temporary destination (G_1) on the line in the free space which is nearest to the point (V_0). For this temporary destination, the planner repeats the same operation until a safe circular path is found (try arc $P_0 V_1 G_1$, select G_2 , and find $P_0 G_2$). If a path is found but the endpoint of the path is a selected via points,

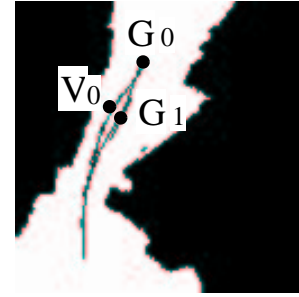


Figure 11. A path planning result.

this process is iterated with the selected via point (G_2) being the initial position and the original destination (G_0) as the destination. Currently we limit the maximum iteration of this process to two; in a complex environment, the endpoint of the planned path may not be the destination.

The obstacle region in Fig. 9 is made by expanding the original obstacle region by two types of margins; one is for considering the motion uncertainty (currently set to $20[cm]$); the other is for considering the size of the robot. Since the shape of the horizontal section of our robot is rectangle, we use as the margin a half of the width of the robot. However, since this margin may not be appropriate depending on the relative position of the robot and an obstacle, the planner verifies the safety of a path by checking collision on every point on the path using the robot shape, as shown in Fig. 10. If the collision is detected on the path, the planner goes back to the selection of via points; that is, the planner selects another via point near the previous one but at a further point from the obstacle, and tries to find a feasible path as explained above.

Fig. 11 shows an example of path planning. The point G_0 is the destination, the point V_0 is the point on the initial circular path towards G_0 which is farthest from the free space, and the point G_1 is the selected temporary destination. Note that the black regions are the original occupied ones and are not expanded by the motion uncertainty nor the robot's half width.

6 Navigation Experiment

Fig. 12 shows a navigation result. In Fig. 12, the robot began moving from the start point, moved along the arrow shown in the figure, and finally arrived at the goal point. The observation cycle is $0.4[sec]$ and the robot's maximum speed is $1.0[m/s]$. Fig. 13 shows snapshots of the navigation experiment.

Fig. 14 shows free space maps and planned paths in the navigation. At point (a), the planned path was long enough to enable the robot to move fast. At point (b), since the observed area was narrow, the robot could plan only a short path and slowed down. At point (c), the robot could observe a wide area, so it moved fast again. At point (d), similar to the case at point (b), the robot slowed down. The total moving distance was about $30[m]$ and the total time was about $45[sec]$.

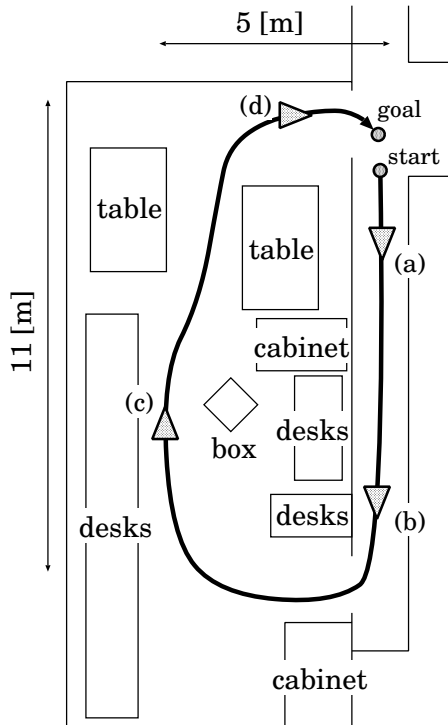


Figure 12. A navigation result.

7 Conclusion

This paper has proposed a method of controlling the robot speed based on the distance to undecided regions in a probabilistic occupancy map. From the models of observation uncertainty and data integration, we derive the number of observations needed to make a target region be free with confidence. This number is then used to determine the maximum safe speed. The method has been successfully applied to a mobile robot navigation in an unknown environment.

Currently we treat the reliability of *undecided* regions uniformly; that is, the necessary number of observation is the same for every undecided regions. The reliability of each grid, however, should differ from each other depending on the observation history of the grid. A future work is to consider this factor in speed control. Another future work is to integrate the proposed strategy with the motion control based on the size of the nearby free space [7]. In the current experiments, we deal with only the situation where the nearby free space is sufficiently large. By this integration, a safe and efficient navigation will be realized in various environments.

References

- [1] W. Burgard, D. Fox, and S. Thrun. Active mobile robot localization. *Proc. IJCAI-97*, pages 1346–1352, 1997.
- [2] H. Choset, J. Burdick, S. Walker, and K. Eiamsa-Ard. Sensor based exploration: Incremental construction of the hierarchical generalized voronoi graph. *Int. J. of Robotics Research*, 19(2):126–148, 2000.
- [3] A. Elfes. Sonar-based real-world mapping and navigation. *Int. J. of Robotics and Automat*, 3(3):249–265, 1987.

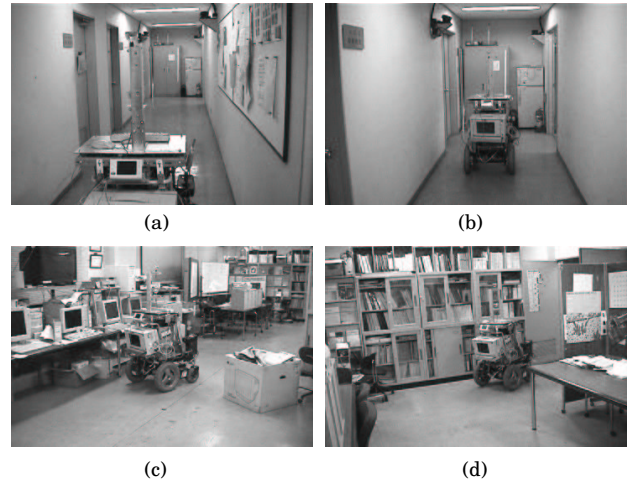


Figure 13. Snapshots of a navigation experiment.

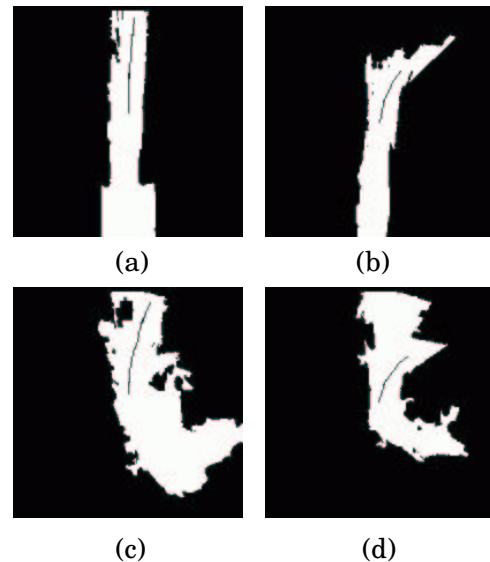


Figure 14. Free space maps and planned paths.

- [4] H. Koyasu, J. Miura, and Y. Shirai. Realtime omnidirectional stereo for obstacle detection and tracking in dynamic environments. *Proc. of IROS-01*, pages 31–36, 2001.
- [5] J. Leonard and H. Durrant-Whyte. Simultaneous map building and localization for an autonomous mobile robot. *Proc. of IROS-91*, pages 1442–1447, 1991.
- [6] J. Miura, Y. Negishi, and Y. Shirai. Mobile robot map generation by integrating omnidirectional stereo and laser range finder. *Proc. of IROS-02*, pages 250–255, 2002.
- [7] I. Moon, J. Miura, and Y. Shirai. On-line viewpoint and motion planning for efficient visual navigation under uncertainty. *Robotics and Autonomous Systems*, 28(2-3):237–248, 1999.
- [8] S. Thrun. Learning occupancy grids with forward models. *Proc. of IROS-01*, pages 1676–1681, 2001.
- [9] S. Thrun, W. Burgard, and D. Fox. A probabilistic approach to concurrent mapping and localization for mobile robots. *Machine Learning*, 31:29–53, 1998.